

A Phosphorus-Containing Inorganic Compound as an Effective Flame Retardant for Glass-Fiber-Reinforced Polyamide 6

Bin Zhao, Zhi Hu, Li Chen, Yun Liu, Ya Liu, Yu-Zhong Wang

Center for Degradable and Flame-Retardant Polymeric Materials, National Engineering Laboratory of Eco-Friendly Polymeric Materials, College of Chemistry, State Key Laboratory of Polymer Materials Engineering, Sichuan University, Chengdu 610064, China

Received 29 January 2010; accepted 26 April 2010

DOI 10.1002/app.32860

Published online 1 September 2010 in Wiley Online Library (wileyonlinelibrary.com).

ABSTRACT: A novel inorganic compound, aluminum hypophosphite (AP), was synthesized successfully and applied as a flame retardant to glass-fiber-reinforced polyamide 6 (GF-PA6). The thermal stability and burning behaviors of the GF-PA6 samples containing AP (flame-retardant GF-PA6) were investigated by thermogravimetric analysis, vertical burning testing (with a UL-94 instrument), limiting oxygen index (LOI) testing, and cone calorimeter testing (CCT). The thermogravimetric data indicated that the addition of AP decreased the onset decomposition temperatures, the maximum mass loss rate (MLR), and the maximum-rate decomposition temperature of GF-PA6 and increased the residue chars of the samples.

Compared with the neat GF-PA6, the AP-containing GF-PA6 samples had obviously improved flame retardancy: the LOI value increased from 22.5 to 30.1, and the UL-94 rating went from no rating to V-0 (1.6 mm) when the AP content increased from 0 to 25 wt % in GF-PA6. The results of CCT reveal that the heat release rate, total heat release, and MLR of the AP-containing GF-PA6 samples were lower than those of GF-PA6. Furthermore, the higher additive amount of AP affected the mechanical properties of GF-PA6, but they remained acceptable. © 2010 Wiley Periodicals, Inc. *J Appl Polym Sci* 119: 2379–2385, 2011

Key words: composites; flame retardance; polyamides

INTRODUCTION

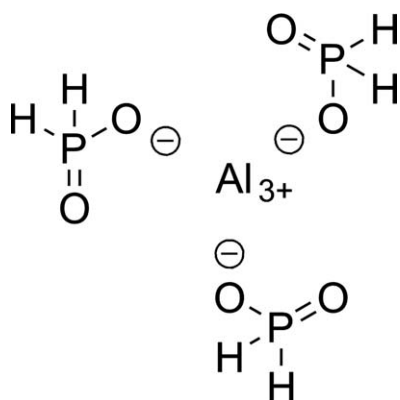
Polyamide 6 (PA6), especially glass-fiber-reinforced polyamide 6 (GF-PA6), has widely been used in many fields, such as in the electrical and electronic industries, because of its higher heat-transition temperature and outstanding mechanical properties.^{1–3} However, both PA6 and GF-PA6 are flammable; this restricts their applications in some fields. The flame retardation of GF-PA6 is much more difficult than that of PA6 because of the candlewick effect caused by the glass fibers (GFs).^{3–5} Thus, the flame retardation of GF-PA6 used in electrical and electronic equipment has been a topical challenge for a long time.³ Many attempts to flame-retard GF-PA6 with some halogen-containing and nonhalogen flame retardants have been reported.^{3–6} Inorganic compounds such as $Mg(OH)_2$ and $Al(OH)_3$ are the most environmentally friendly and cost-effective. However, because of their low efficiency in flame retard-

ance, the additive amounts are high, 50–60 wt %, which results in a deterioration of the mechanical properties of the resulting materials.^{7–9} Nitrogen- and phosphorus-containing flame retardants also show good effects on flame-retardant GF-PA6.^{10–12} Red phosphorus is an efficient halogen-free flame retardant, but it limits the color of the products.^{6,10} Melamine polyphosphate contains both phosphorus and nitrogen, which combine the flame-retardant mechanisms of both gaseous and condensed phases. It can be used as an intumescent flame retardant for GF-PA6 because of its special flame-retardant mechanism.^{3,11,12} However, GF-PA6 cannot reach an optimal flame-retardant level through the addition of melamine polyphosphate at a low content. A series of colorless, organophosphinates have been successfully introduced into PA since 2002 by Clariant, such as Exolit OP 1312 and 1310, which can give good flame retardancy to GF-PA6.^{11–14} According to some patents, organophosphinates can also be combined with some nitrogen-containing flame retardants for a P–N synergistic effect.¹⁵ However, the Exolit OP series of flame retardants have high costs because of the complicated synthesis route of the organic phosphinate.

In this study, a low-cost inorganic hypophosphite named *aluminum hypophosphite* (AP) was prepared in

Correspondence to: Y.-Z. Wang (yzwang@scu.edu.cn).

Contract grant sponsor: Key Project of the National Science Foundation of China; contract grant number: 50933005.



Scheme 1 Chemical structure of AP.

our laboratory according to the previous literature.¹⁶ Flame-retardant GF-PA6s with various contents of AP were prepared, and the thermal stability, UL-94 ratings, limiting oxygen index (LOI) values, and cone calorimeter testing (CCT) results were studied comprehensively.

EXPERIMENTAL

Materials

Sodium hypophosphite ($\text{NaH}_2\text{PO}_2 \cdot \text{H}_2\text{O}$, A.R.) and aluminum chloride hexahydrate ($\text{AlCl}_3 \cdot 6\text{H}_2\text{O}$, A.R.) were provided by Kelong Chemical Reagent Factory (Chengdu, China). Commercial PA6 pellets (Aklon F223-D) and GFs were supplied by DSM Engineering Plastics Co. (Shanghai, China).

Synthesis of AP

As provided in the literature on the synthesis of AP,¹⁶ our typical synthetic procedure was as follows: 50.88 g (0.48 mol) of $\text{NaH}_2\text{PO}_2 \cdot \text{H}_2\text{O}$ and 30 mL of deionized water were added to a 250-mL, three-necked flask, and then, the mixture was stirred for 15 min at 50°C. After the solution became transparent, the temperature of the system was elevated to 80–90°C over 30 min. The solution, which contained 38.54 g (0.16 mol) of $\text{AlCl}_3 \cdot 6\text{H}_2\text{O}$, was dropped into the reaction mixture slowly, and then, a white precipitate appeared. The reaction system was stirred at the same temperature for 1 h, and then, the target product was filtered at room temperature, washed with distilled water, and dried to a constant weight in a vacuum oven at 100°C. AP [$\text{Al}(\text{H}_2\text{PO}_2)_3$; 94%], as a white solid, was obtained.

IR (KBr, cm^{-1}): 2408, 2384, 1077, 1187, 829. Anal. Calcd for $\text{Al}(\text{H}_2\text{PO}_2)_3$: Al, 12.2 wt %; P, 41.9 wt %. Found in Inductively coupled plasma atomic emission spectroscopy (ICP-AES): Al, 12.0 wt %; P, 40.0 wt %.

The particle size of AP was about 30–40 μm (99% through a 400-mesh sieve). The chemical structure of AP is presented in Scheme 1.

Preparation of the flame-retardant samples

The flame-retardant PA6 composites were prepared by the mixture of PA6 with GF and AP at various ratios. In all of the reinforced samples, the content of the GF was 30 wt %. After they were stirred in a high-speed mixer, all of the samples were extruded by a twin-screw extruder (SL-J-25-05, Longchang, China), respectively. The composites were cut into pellets and dried for 4 h at 100°C *in vacuo*. Then, all of the samples were compression-molded at 10 MPa for 3 min at 240°C to make them into standard samples required for the corresponding tests. The compositions and designations of the studied materials are listed in Table I.

Thermogravimetric analysis (TGA)

The thermogravimetry (TG) data were obtained on a TG 209F1 TG analyzer (Netzsch, Selb, Germany). All of the samples (ca. 5 mg in weight) were heated from 40 to 700°C at a heating rate of 10°C/min under flowing nitrogen and air at 60 mL/min, respectively. The temperature of the instrument was replicable to within $\pm 0.1^\circ\text{C}$, and the mass was reproducible to within ± 1 wt %.

Tests of flammability

The LOI values were measured by an HC-2C oxygen index meter (Jiangning, Nanjing, China) with $130 \times 6.5 \times 3.0$ mm³ bars according to ASTM D 2863-97.

The vertical burning experiments were done on a vertical burning test instrument (CZF-2-type, Jiangning, Nanjing, China) with $130 \times 13 \times 3.0$ mm³ and $130 \times 13 \times 1.6$ mm³ bars, respectively, according to ASTM D 3801.

CCT was conducted on an FTT cone calorimeter (FTT, East Grinstead, UK) at an incident heat flux of 50 kW/m² according to the conditions of the procedure listed in ISO 5660-1. The tests were carried out on square specimens (100 × 100 × 6 mm³).

TABLE I
Weight Ratio Compositions of the Studied Materials

Sample	PA6	GF	AP	Antioxidants
GF-PA6	69.5	30	—	0.5
GF-PA6/AP10	59.5	30	10	0.5
GF-PA6/AP15	54.5	30	15	0.5
GF-PA6/AP20	49.5	30	20	0.5
GF-PA6/AP25	44.5	30	25	0.5

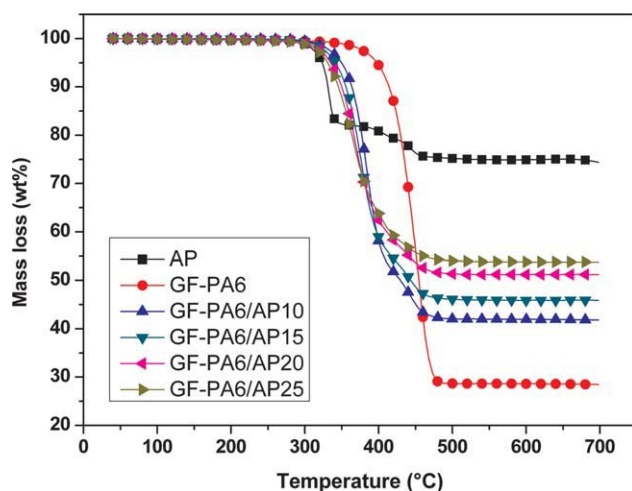


Figure 1 TG curves of AP, GF-PA6, and GF-PA6 with different contents of AP in N₂. [Color figure can be viewed in the online issue, which is available at wileyonlinelibrary.com.]

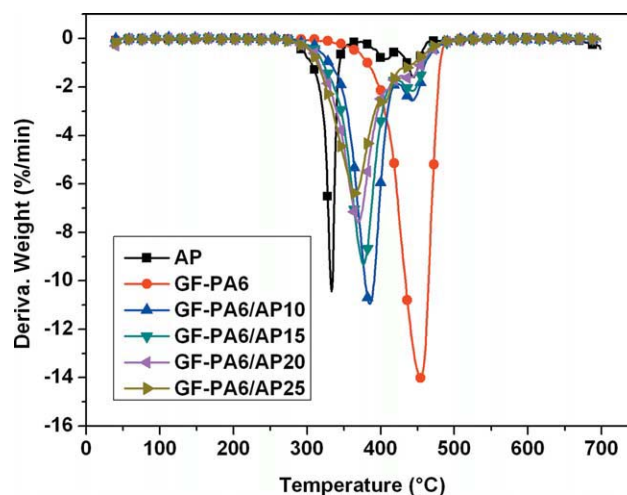


Figure 2 DTG curves of AP, GF-PA6, and GF-PA6 with different contents of AP in N₂. [Color figure can be viewed in the online issue, which is available at wileyonlinelibrary.com.]

Tensile tests were completed in accordance with the procedures in GB/T 1040-2006 at a crosshead speed of 50 mm/min. The flexural properties were measured in accordance with the procedures in GB/T 9314-2000 at a crosshead speed of 2 mm/min and a span width of 64 mm. The Izod impact properties were tested in accordance with the procedures in GB/T 1843-2008, and the depth of the nick was 2 mm.

RESULTS AND DISCUSSION

Thermal decomposition behaviors

To understand the thermal stability and decomposition behavior of the flame-retardant GF-PA6, TGA of GF-PA6 and GF-PA6 with different contents of AP was carried out in nitrogen and air atmospheres at a heating rate of 10°C/min from 40 to 700°C. TGA and differential thermogravimetry (DTG) curves obtained under nitrogen are shown in Figures 1 and 2, respectively, and the corresponding data are presented in

Table II. The thermal decomposition of GF-PA6 was revealed by a single degradation step with a maximum mass loss rate (MLR) at 454.1°C; this resulted in the release of water, carbon monoxide, carbon dioxide, ammonia and its derivatives, and hydrocarbon fragments.¹⁷ The char residue at 700°C was 28.5 wt %, which resulted from the GFs added.² When AP was added, there appeared to be regular changes in the thermal stability and the decomposition behaviors. On the one hand, the data obtained from TGA indicated that the addition of AP decreased both the onset decomposition temperatures (T_{onset} 's; ca. 50–70°C below that of the neat GF-PA6) and the maximum-rate decomposition temperatures (T_{max} 's) of the samples; this was attributed to two aspects. First, the TG data revealed that AP itself exhibited a lower thermal stability than GF-PA6; second, the catalytic activity for the aromatization of the PA6 matrix induced by the metal hypophosphite as a weak Lewis acid–base interaction with the matrix may have further reduced the thermal stability of the flame-retardant

TABLE II
Main TG and DTG Data of the Samples in Nitrogen

Sample	T_{onset} (°C) ^a	$T_{\text{max}1}$ (°C)	$T_{\text{max}2}$ (°C)	MLR at $T_{\text{max}1}$ (wt %/min)	Residues at 700°C (wt %)	Normalized residues (wt %)
AP	323.3	333.2	444.6	10.5	74.4	0
GF-PA6	397.6	454.1 ^b		14.0	28.5	0
GF-PA6/AP10	349.8	385.7	444.1	11.0	41.8	5.9
GF-PA6/AP15	341.2	376.7	444.2	9.4	45.9	6.2
GF-PA6/AP20	335.1	369.3	437.8	7.6	51.2	7.8
GF-PA6/AP25	330.9	365.2	434.0	6.4	53.8	6.7

^a T_{onset} indicates the point of 5% weight loss.

^b GF-PA6 exhibited a single degradation step in TGA.

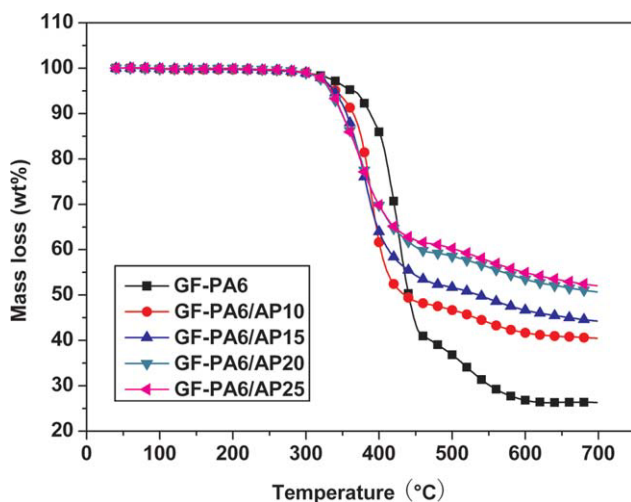


Figure 3 TG curves of GF-PA6 and GF-PA6 with different contents of AP in air. [Color figure can be viewed in the online issue, which is available at wileyonlinelibrary.com.]

specimens.¹⁸ On the other hand, there appeared to be two peaks in the DTG curves of the flame-retardant samples, as shown in Figure 2. As shown by a comparison of the DTG curves of GF-PA6 and the GF-PA6/APs, AP decreased the maximal MLR remarkably by interfering with the main decomposition of the matrix with regard to the flame-retardant constituents in the temperature range 365–385°C. The first peak was related to the degradation of AP and the chemical/catalytic interaction between AP and PA6. However, the second degradation step was attributed to the further decomposition and charring of the remnant PA6 matrix, which was not affected by the flame retardant,¹⁹ and the rate of mass loss (ML) was further decreased with increasing AP. For the GF-PA6/AP specimens, with the mass fraction of the GF remnant (ca. 28.5 wt %) from the reference results of GF-PA6 and AP residues mostly on an aluminum oxide basis

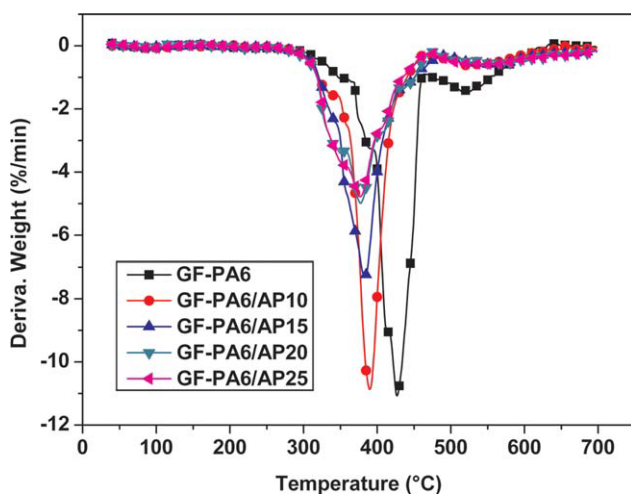


Figure 4 DTG curves of GF-PA6 and GF-PA6 with different contents of AP in air. [Color figure can be viewed in the online issue, which is available at wileyonlinelibrary.com.]

TABLE III
Main TG and DTG Data of the Samples in Air

Sample	T_{onset} (°C) ^a	T_{max1} (°C)	T_{max2} (°C)	MLR at		Residues at 700°C (wt %)
				T_{max1} (wt %/min)	T_{max2} (wt %/min)	
GF-PA6	364.1	426.8	518.8	11.0		26.3
GF-PA6/AP10	340.6	390.0		11.1		40.5
GF-PA6/AP15	338.2	383.2		7.3		44.3
GF-PA6/AP20	332.7	377.3		4.9		50.7
GF-PA6/AP25	334.1	376.8		4.7		52.1

^a T_{onset} indicates the point of 5% weight loss.

(ca. 74.4 wt %), the char yields of the flame-retardant specimens were higher than the total content of the inorganic additives (the normalized residues are listed in Table II); this indicated that during heating, a certain content of PA6 fragment was preserved as a result of charring induced in the presence of AP.

The TGA and DTG curves obtained under air are shown in Figures 3 and 4, respectively, and the corresponding data are presented in Table III. Similar thermal degradation behavior between the nitrogen and air atmospheres was observed. The data obtained from TGA indicated that the addition of AP decreased both T_{onset} (by approximately 20–30°C) and T_{max} of the samples. However, the thermal decomposition of GF-PA6 was revealed by two degradation steps with maximum MLRs at 426.8 and 518.8°C in air but by a single degradation step in a nitrogen atmosphere. The second degradation step was attributed to the further decomposition and charring of the remnant PA6 matrix. The flame-retardant samples showed similar thermal decomposition behaviors in both nitrogen and air.

Flame retardancy

The LOI and UL-94 test results of GF-PA6 with different contents of AP are listed in Table IV. The LOI value of GF-PA6 was only 22.5. When AP was added to GF-PA6 as a flame retardant, the LOI values increased obviously, and a V-0 rating at 3.0 mm in the UL-94 standard was obtained when the flame-retardant content reached 20 wt %. Furthermore, a V-0 rating at 1.6 mm was achieved when the content of AP

TABLE IV
Flame Retardancy of the GF-PA6 Materials with Different AP Contents

Specimen	Phosphorus content (wt %)	LOI (%)	UL-94 rating (3.0 mm)	UL-94 rating (1.6 mm)
GF-PA6	0	22.5	NR	NR
GF-PA6/AP10	4.19	24.3	NR	NR
GF-PA6/AP15	6.28	25.2	NR	NR
GF-PA6/AP20	8.37	27.5	V-0	NR
GF-PA6/AP25	10.47	30.1	V-0	V-0

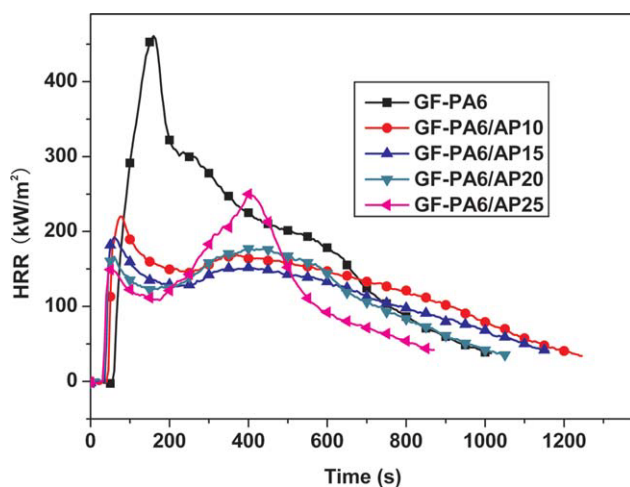


Figure 5 HRR curves of GF-PA6 and GF-PA6 with different contents of AP. [Color figure can be viewed in the online issue, which is available at wileyonlinelibrary.com.]

reached 25 wt % in the flame-retardant samples. The highest LOI value we reached was 30.1 in the samples studied, which was approximately 34% higher than that of the neat GF-PA6. Generally, the phosphorus content is a crucial factor in the efficiency of a halogen-free flame retardant, particularly for aliphatic polyamides.²⁰ In this study, the phosphorus content of AP was 41.9 wt %, which was higher than that of many organic halogen-free flame retardants, which was the reason for the increases in the LOI values and the UL-94 rating of the flame-retardant GF-PA6.

Cone calorimeter

The cone calorimeter is a useful instrument for fire safety researchers who are interested in the quantitative flammability analysis of materials.²¹ The results of cone calorimeter investigations are a comprehensive characterization of the performance of the tested samples in a rather well-defined fire test scenario.²² To understand the function of AP as a phosphorus-containing flame retardant added to GF-PA6, CCT was carried out.

Heat release rate (HRR) and time to ignition (TTI)

HRR is considered to have the most important influence on the fire hazard, and it is a measure of the heat

release per unit of surface area of a burning material.²³ The HRR plots for each sample at an incident heat flux of 50 kW/m² are presented in Figure 5 for comparison, and the complete CCT data are summarized in Table V. GF-PA6 burned quickly after ignition, and an intensive peak turned up with a peak heat release rate (PHRR) value of 460 kW/m² at 160 s; this was followed by a sudden decrease in HRR with time, which was a characteristic HRR behavior for GF-reinforced materials.²⁴ When AP was added, the PHRR values of the flame-retardant GF-PA6 were distinctly reduced, and the curves showed an increase in the total burning time compared with that of GF-PA6. In other words, this means that the flame-retardant GF-PA6 burned for a longer time with a flame weaker than that of neat GF-PA6, which indicated that the flame-retardant GF-PA6 samples exhibited more difficulty in ignition and propagation of flame than the neat GF-PA6. The HRR curves of flame-retardant GF-PA6 were much lower and flatter than that of GF-PA6, which is typical for a residue-forming material.² The flame-retardant materials, in particular the samples containing more APs, showed a second PHRR in later stages of combustion. This phenomenon was caused by the cracking char or the pyrolysis of the remnant AP.²⁵ Another obvious change was the decrease in TTI between the neat and flame-retardant samples; this was in agreement with the TG test. The reduction of TTI might have been due to the initial combustion of flame retardants before these could play their role in the materials.²⁶ Few studies have been carried out on the relationship between TTI and HRR, but the correlation in Table V could be explained on the basis of an early ignition that allowed a lower accumulation of combustible vapors to give rise to the reduction of HRR after ignition.²⁷ The fire growth rate (FIGRA) as a necessary parameter, which was calculated from the measured data of CCT and defined as the ratio of PHRR to the time at which PHRR was reached (t_p), indicated the burning propensity of the materials.²⁸ GF-PA6 had a FIGRA value of 2.88. At lower AP contents, the FIGRA values first increased because of the t_p of GF-PA6/APs being substantially ahead of that of the neat GF-PA6 sample. When the AP content was further increased, the flame-retardant level achieved with AP, measured by the FIGRA index, was notable; this was ascribed to both

TABLE V
Combustion Parameters Obtained from the Cone Calorimeter

Specimen	PHRR (kW/m ²)	TTI (s)	t_p (s)	FIGRA (kW/s m ²)	THR (MJ/m ²)	Residual char (%)
GF-PA6	460	53	160	2.88	180	30
GF-PA6/AP10	220	35	80	2.93	158	42
GF-PA6/AP15	192	32	60	3.20	128	47
GF-PA6/AP20	177	28	405	0.44	122	54
GF-PA6/AP25	249	27	405	0.61	106	60

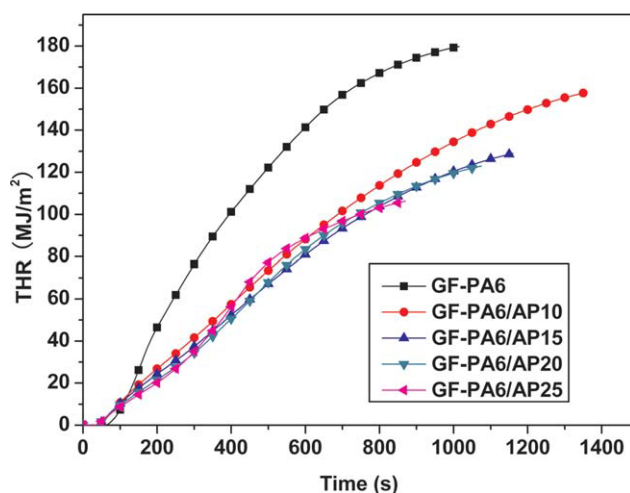


Figure 6 THR curves of GF-PA6 and GF-PA6 with different contents of AP. [Color figure can be viewed in the online issue, which is available at wileyonlinelibrary.com.]

the decrease of PHHR and the prolongation of t_p . The decrease in the FIGRA values with the addition of AP meant that the GF-PA6/APs had a higher fire safety than neat GF-PA6. Low FIGRA values indicate a delayed time to flashover, which allows enough time for evacuation and survival.²⁹

Total heat release (THR)

An obvious decreasing trend was observed between the neat sample and the flame-retardant samples on THR, as shown in Table V and Figure 6. The neat sample released a total heat of 180 MJ/m², whereas THR was reduced in proportion to AP contents of 10, 15, 20, and 25 wt % by approximately 12, 29, 32, and 41%, respectively. The reason for that was that the residue formation of the flame-retardant materials partly cut off the heat transfer in combustion. These lower THR data indicated that AP was an effective flame retardant, which retarded combustion of the materials.

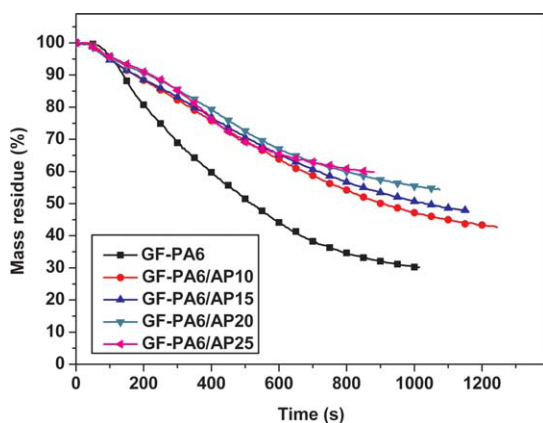


Figure 7 ML curves of GF-PA6 and GF-PA6 with different contents of AP. [Color figure can be viewed in the online issue, which is available at wileyonlinelibrary.com.]

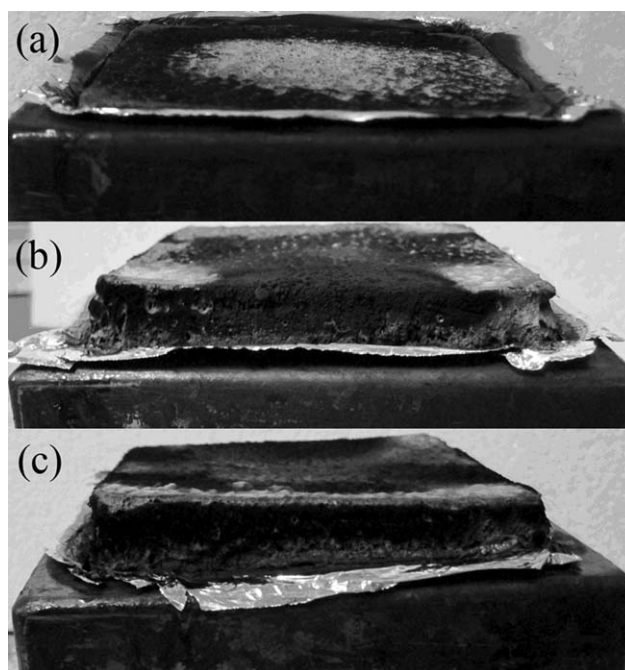


Figure 8 Digital photographs of the residue chars after CCT: (a) GF-PA6, (b) GF-PA6/AP20, and (c) GF-PA6/AP25.

Mass loss (ML)

ML is a factor which plays a vital role in the combustion of a polymer. Figure 7 presents the mass residue values measured as a function of time. As shown in Table V and Figure 7, when more AP was added to the materials, a larger amount of char was formed at the end of combustion, and a lower MLR was obtained. Correspondingly, digital photographs of the residue chars after CCT are presented in Figure 8. Compared with GF-PA6, the flame-retardant GF-PA6 samples formed thicker and more compact residue chars at the end of the combustion, which prevented the mass/heat transfer. AP was a cost-effective flame retardant, which disposed of the candlewick effect of GF-PA6 effectively, and the GFs played a positive role in flame retardancy because of the increased strength of residual chars and reduced thermal decomposition rate.³⁰ Therefore, GFs served as an antidripping agent in GF-PA6, which promoted the formation of thick and compact residual chars when the materials burned.³¹

Mechanical properties

The mechanical properties, including the tensile properties, flexural properties, and notched Izod impact strength, of neat GF-PA6, GF-PA6/AP20, and GF-PA6/AP25 are presented in Table VI. With increasing AP content in the composites, the tensile strength, elongation at break, flexural strength, and

TABLE VI
Mechanical Properties of Neat GF-PA6, GF-PA6/AP20,
and GF-PA6/AP25

Specimen	GF-PA6	GF-PA6/AP20	GF-PA6/AP25
Tensile strength (MPa)	160.6	150.7	139.5
Elongation at break (%)	14.9	12.6	11.5
Flexural strength (MPa)	196.8	196.0	161.3
Notched Izod impact strength (kJ/m ²)	9.7	7.3	5.3

impact toughness of the composites decreased, especially for the GF-PA6/AP25 specimen. The tensile strength, elongation at break, flexural strength, and impact toughness of GF-PA6/AP20 were 150.7 MPa, 12.6%, 196.0 MPa, and 7.3 kJ/m², respectively; these values correspondingly decreased by 6.2, 15.4, 0.4, and 24.7%, respectively, compared with those of the neat GF-PA6. We concluded that the higher additive amount of AP affected the mechanical properties of GF-PA6, but they were still acceptable, and the additive amount of 20 wt % was suitable according to the balance of the flame retardancy and mechanical properties of the composites compared with those of the neat GF-PA6.

CONCLUSIONS

The inorganic compound AP was an effective flame retardant for GF-PA6 because of its high phosphorus content (41.9 wt %). The TGA results indicate that the thermal stability and the decomposition behavior of GF-PA6 were both changed with the addition of AP; this resulted from the low thermal stability and the catalytic activity of AP. The cone calorimeter results indicated that the addition of AP significantly reduced HRR, THR, and MLR of the flame-retardant samples compared with the neat GF-PA6. The flame-retardant GF-PA6 samples showed typical behavior of residue-forming materials and a higher safety rank. The residual char of the flame-retardant GF-PA6 after CCT was more compact and stronger than that of the neat GF-PA6. Compared with the neat GF-PA6, the flame-retardant GF-PA6 samples had an improved UL-94 rating, for example, going from no rating (NR) for the neat GF-PA6 to V-0 (1.6 mm) for the GF-PA6 containing 25 wt % AP. Meanwhile, the LOI value also

increased from 22.5 to 30.1. Moreover, the mechanical properties of GF-PA6/20 almost remained the same as the neat GF-PA6, only decreasing a little. All of the results reveal that AP was a cost-effective flame retardant for GF-PA6, whereas the dominant fire-retardant mechanisms must be investigated adequately; these results will be reported in another article.

References

- Weil, E. D.; Levchik, S. V. *J Fire Sci* 2004, 22, 251.
- Ulrike, B.; Bernhard, S.; Mario, A. F. *Polym Degrad Stab* 2007, 92, 1528.
- Chen, L.; Wang, Y. Z. *Polym Adv Technol* 2010, 21, 1.
- Gunduz, H. O.; Isitman, N. A.; Aykol, M.; Kaynak, C. *Polym Plast Technol Eng* 2009, 48, 1046.
- Isitman, N. A.; Gunduz, H. O.; Kaynak, C. *Polym Degrad Stab* 2009, 94, 2241.
- Isitman, N. A.; Gunduz, H. O.; Kaynak, C. *J Fire Sci* 2010, 28, 87.
- Li, M. M.; Chen, Y. H.; Wang, Q. *Polym Mater Sci Eng* 2006, 22, 241.
- Ou, Y. X. *Applied Flame-Retarding Technology*; Chemical Industrial Press: Beijing, 2002.
- Fei, G. X.; Liu, Y.; Wang, Q. *Polym Degrad Stab* 2008, 93, 1351.
- Markarian, J. *Plast Addit Compd* 2005, 7, 22.
- Levchik, S. V.; Weil, E. D. *J Fire Sci* 2006, 24, 346.
- Jahromi, S.; Gabrielse, W.; Braam, A. *Polymer* 2003, 44, 25.
- Weferling, N.; Schmitz, H.-P. U.S. Pat. 6,242,642 B1 (2001).
- Hoerold, S. U.S. Pat. 6,420,459 B1(2002).
- Silvestro, C.; Maurizio, L. U.S. Pat. 2008/0033079 A1 (2008).
- Everest, D. A. *J Chem Soc* 1952, 2945.
- Hornsby, F. R.; Wang, J.; Rothon, R.; Jackson, G.; Wilkinson, G.; Cossick, K. *Polym Degrad Stab* 1996, 51, 235.
- Afshari, M.; Gupta, A.; Jung, D.; Kotek, R.; Tonelli, A. E.; Vasanthan, N. *Polymer* 2008, 49, 1297.
- Ma, H.; Fang, Z.; Tong, L. *Polym Degrad Stab* 2006, 91, 1972.
- Levchik, S. V.; Weil, E. D. *Polym Int* 2000, 49, 1033.
- Morgan, A. B.; Bundy, M. *Fire Mater* 2007, 31, 257.
- Schartel, B.; Bartholmai, M.; Knoll, U. *Polym Degrad Stab* 2005, 88, 540.
- Liu, Y.; Wang, J. S.; Deng, C. L.; Wang, D. Y.; Song, Y. P.; Wang, Y. Z. *Polym Adv Technol*, DOI: 10.1002/pat.1502.
- Casu, A.; Camino, G.; DeGiorgi, M.; Flath, D.; Laudi, A.; Morone, V. *Fire Mater* 1998, 22, 7.
- Schartel, B.; Hull, T. R. *Fire Mater* 2007, 31, 327.
- Gallina, G.; Bravin, E.; Badalucco, C.; Audisio, G.; Armanini, M.; Chirico, A. D.; Provasoli, F. *Fire Mater* 1998, 22, 15.
- Babrauskas, V. Y.; Parker, W. J. *Fire Mater* 1987, 11, 31.
- Bourbigot, S.; Devaux, E.; Flambard, X. *Polym Degrad Stab* 2002, 75, 397.
- He, S. Q.; Hu, Y.; Song, L.; Tang, Y. *J Fire Sci* 2007, 25, 109.
- Jou, W. S.; Chen, K. N.; Chao, D. Y.; Lin, C. Y.; Yeh, J. T. *Polym Degrad Stab* 2001, 74, 239.
- Liu, Y.; Deng, C. L.; Zhao, J.; Wang, J. S.; Chen, L.; Wang, Y. Z. *Polym Degrad Stab*, DOI: 10.1016/j.polymerdegradstab.2010.02.03310.